

# A Novel Massively Parallel Computing Method for Fluid-Structure Coupling Analysis

Kazuyasu Sugiyama<sup>1,2</sup>, Satoshi Ii<sup>3</sup>, Shu Takagi<sup>1,2</sup>, and Yoichiro Matsumoto<sup>1</sup>

<sup>1</sup>School of Engineering, The University of Tokyo, Japan

<sup>2</sup>RIKEN Computational Science Research Program, Japan

<sup>3</sup>Department of Mechanical Science and Bioengineering, Osaka University, Japan

## 1 Introduction

Numerical simulations of Fluid-Structure Interaction (FSI) problems have been expected to afford much insight into biological and biomedical systems along with recent advances in high-performance computing. Unlike conventionally-used Lagrangian methods with a mesh generation/reconstruction procedure, the authors have developed an Eulerian method using fixed regular grids [1]–[6]. It facilitates simulations of systems involving a large number of dispersed bodies, and avoids a breakdown in a large deformation owing to the absence of the mesh distortion problem. In view of computational efficiency, the monolithic formulation readily gets great performance out of SIMD processing and makes a workload on each compute core equivalent. It allows us to utilize efficient algorithms cultivated for incompressible fluid flow problems. Nevertheless, an iterative procedure for solving the pressure Poisson equation makes it difficult to exploit the system performance on a recent scalar supercomputer because the performance of the solver is limited by the memory bandwidth and repetitive communications rather than the floating-point operation speed. Following a revived Artificial Compressibility Method (ACM) [7], the authors have been developing a novel algorithm to drastically enhance the efficiency and scalability. We will demonstrate its validity and usefulness for the Eulerian FSI simulation.

## 2 Numerical methods

### 2.1 On Eulerian description

As in many analyses for biological systems, the fluid and solid phases are assumed to be incompressible. The governing equations consist of mass and momentum conservations. The basic equations are discretized on a fixed Cartesian mesh in a finite-difference manner. The hyperelastic dynamics is incorporated into a standard incompressible flow solver to realize the fluid-structure coupling analysis. Here, we shall focus on an evaluation of the stress tensor, which is a key issue in the Eulerian formulation. For more detailed description, see [2].

In the Lagrangian method, the fluid and solid phases are distinguished by the boundary fitted mesh, and the level of solid deformation is quantified by the relative change in the adjacent material points. By contrast, in the present Eulerian method [2], to represent the kinematics of structure, the solid volume fraction  $\phi_s$  and the left Cauchy-Green deformation tensor  $\mathbf{B}$  are defined on each grid point, and temporally updated by solving transport equations

$$\partial_t \phi_s + \mathbf{v} \cdot \nabla \phi_s = 0, \quad (1)$$

$$\partial_t \mathbf{B} + \mathbf{v} \cdot \nabla \mathbf{B} = \mathbf{L} \cdot \mathbf{B} + \mathbf{B} \cdot \mathbf{L}^L, \quad (2)$$

where  $\mathbf{v}$  denotes the velocity vector, and  $\mathbf{L}(= \nabla \mathbf{v}^T)$  the velocity gradient tensor. The Cauchy stress tensor  $\boldsymbol{\sigma}$  is written in a fluid-solid mixture form. For example, a system consisting of Newtonian fluid and neo-Hookean material obeys

$$\boldsymbol{\sigma} = -P\mathbf{I} + \{(1 - \phi_s)\mu_f + \phi_s\mu_s\}(\mathbf{L} + \mathbf{L}^T) + \phi_s G(\mathbf{B} - \text{tr}(\mathbf{B})\mathbf{I}/3), \quad (3)$$

where  $P$  denotes the pressure,  $\mu$  the viscosity, and  $G$  the modulus of transverse elasticity.

### 2.2 Artificial compressibility method with adaptive parameters

The pressure deviation  $p$  from the driving pressure gradient to pump the system is given to satisfy  $\langle p \rangle = 0$  (here,  $\langle \dots \rangle$  stands for the volume average over the whole computational domain). Following the SMAC algorithm, we introduce the unprojection and projection steps to update the variables. The predicted velocity  $\mathbf{v}^*$  is supposed to be given after the unprojection step. Following [7], we write the incremental pressure  $\delta p (= p^{N+1} - p^N)$  as

$$\delta p = -(CD^* + \Gamma p^N)/(\Delta t), \quad (4)$$

where  $D(= \rho \nabla \cdot \mathbf{v})$  denotes the divergence of the mass flux. At the projection step, the velocity is updated as

$$\mathbf{v}^{N+1} = \mathbf{v}^* - (\Delta t)\rho^{-1}\nabla(\delta p). \quad (5)$$

Although the solenoidal condition ( $\nabla \cdot \mathbf{v} = 0$ ) is not perfectly satisfied in the ACM, it is approximated as exactly as possible. From (4) and (5), we obtain

$$\begin{aligned} \langle (D^{N+1})^2 \rangle &= \langle (D^*)^2 \rangle + 2\langle D^* \nabla^2 D^* \rangle C + \langle (\nabla^2 D^*)^2 \rangle C^2 \\ &+ \langle (\nabla^2 p^N)^2 \rangle \Gamma^2 + 2\langle D^* \nabla^2 p^N \rangle \Gamma + 2\langle (\nabla^2 D^*) (\nabla^2 p^N) \rangle C\Gamma. \end{aligned} \quad (6)$$

Under the condition of  $\Gamma \geq 0$ , the parameters  $C$  and  $\Gamma$  are dynamically determined to minimize  $\langle (D^{N+1})^2 \rangle$ . In a MPI parallelization, the advocated algorithm involves no iterative procedures, and thus considerably reduces the amount of the memory access and adjacent communication. When the second-order finite difference is applied, the pseudo Mach number was found to have an upper limit  $2\sqrt{3}\eta$  (here,  $\eta$  is the CFL number based on the maximum advection speed), guaranteeing the computed velocity field to be nearly incompressible as long as  $\eta$  is sufficiently smaller than unity.

### 3 Results and discussion

To demonstrate the validity of the method, simulated results of a channel flow involving 16 discoid biconcave particles are exemplified. For comparison, two kinds of simulations are performed: one is based on the SMAC algorithm, in which the Fast Fourier Transform (FFT) and the Tri-Diagonal Matrix Algorithm (TDMA) are applied to exactly solving the pressure Poisson equation, while the other is based on the present ACM. The particle position and orientation are shown in Fig. 1. The particles deform and translate in the downstream. As the time goes on, they rotate and tend to be more mixed. There are no significant discrepancies in the particle position and shape between the results based on the SMAC algorithm and present ACM. To further check whether an energy conservation is correctly captured, we report a budget of the overall kinetic-energy transport in Fig. 2. The chained curve in Fig. 2 corresponds to the summation of all the contributions, which should be zero. Its absolute value is much smaller than the variation of the contributions of the individual terms. Therefore, the system is well conserved during the simulation in view of the energy balance, and the energy exchange between the fluid and solid phases via the solid deformation is reasonably guaranteed.

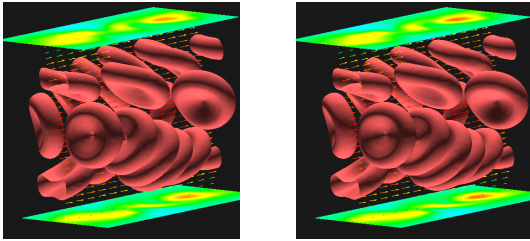


Fig. 1. The snapshots of hyperelastic particles in a three-dimensional Poiseuille flow at  $t = 6.4\text{ms}$ . The computational extent is  $L_x \times L_y \times L_z = 21.12\mu\text{m} \times 21.12\mu\text{m} \times 21.12\mu\text{m}$ , and the number of grid points is  $M_x \times M_y \times M_z = 128 \times 128 \times 128$ . The material properties and the driving pressure gradient are scaled using the density  $\rho$ , and set to  $\mu/\rho = 1 (\mu\text{m})^2/\mu\text{s}$ ,  $G/\rho = 2 \times 10^{-2} (\mu\text{m})^2/(\mu\text{s})^2$  and  $-\Delta P/(\rho L_x) = 2 \times 10^{-4} \mu\text{m}/(\mu\text{s})^2$ . The left and right panels show the results based on the SMAC method using FFT-TDMA and those on the present ACM, respectively. The colors on the walls indicate the magnitude of the shear stress.

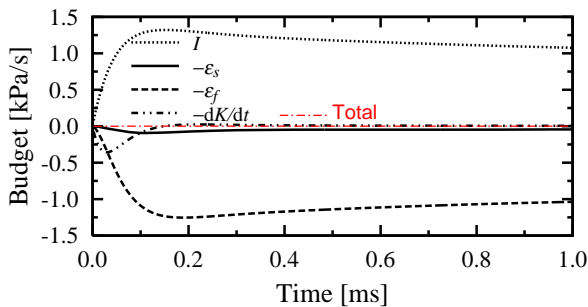


Fig. 2. The budget of the kinetic-energy transport in the Poiseuille flow containing 16 particles using the present ACM. Therein,  $dK/dt$ ,  $I$ ,  $\varepsilon_s$  and  $\varepsilon_f$  denote the kinetic-energy rate, the energy input rate, the strain energy rate, and the kinetic-energy dissipation rate, respectively.

To demonstrate the applicability of the novel formulation and algorithm to massively parallel computing, the FSI simulations in the channel are also performed for various number  $N$  of compute nodes on the K computer. Fixing the problem size per node, we conduct weak scaling tests, and report the performance in Fig. 3. An ex-

cellent scalability is found therein. Notably, the performance ratio is 46.6%, 45.6% and 43.7% for  $N = 1$ ,  $N = 2$  and  $N = 12, 288$ , respectively, revealing unprecedentedly high efficiency among numerical simulations of incompressible fluid/structure dynamics performed on state-of-the-art scalar-type supercomputers.

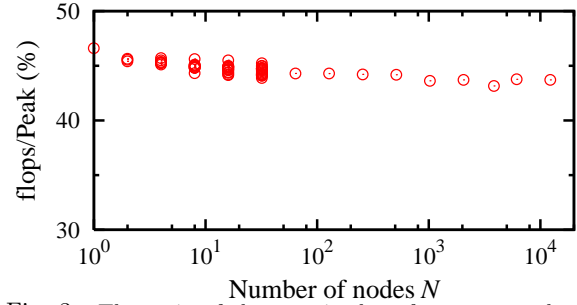


Fig. 3. The ratio of the sustained performance to the peak performance of the K computer as a function of the number  $N$  of compute nodes. The number of grid points per node is  $512 \times 128 \times 128$ .

### 4 Conclusion

A novel numerical method for fluid-structure interaction systems has been developed. It was applied to the three-dimensional simulation of the channel flow including hyperelastic particles. Its validity and also high efficiency and scalability in massively parallel computing were demonstrated.

### Acknowledgment

This research was supported by Research and Development of the Next-Generation Integrated Simulation of Living Matter, a part of the Development and Use of the Next-Generation Supercomputer Project of the Ministry of Education, Culture, Sports, Science and Technology. Part of the results was obtained by early access to the K computer at the RIKEN AICS.

### References

- [1] Sugiyama, K., Ii, S., Takeuchi, S., Takagi, S. and Matsumoto, Y., Full Eulerian simulations of biconcave neo-Hookean particles in a Poiseuille flow, *Comput. Mech.*, **46**, 147–157, 2010.
- [2] Sugiyama, K., Ii, S., Takeuchi, S., Takagi, S. and Matsumoto, Y., A full Eulerian finite difference approach for solving fluid-structure coupling problems, *J. Comput. Phys.*, **230**, 596–627, 2011.
- [3] Ii, S., Sugiyama, K., Takeuchi, S., Takagi, S. and Matsumoto, Y., An implicit full Eulerian method for the fluid-structure interaction problem, *Int. J. Numer. Meth. Fluids*, **65**, 150–165, 2011.
- [4] Takagi, S., Sugiyama, K., Ii, S. and Matsumoto, Y., A review of full Eulerian methods for fluid structure interaction problems, *J. Appl. Mech.*, **79**, 010911, 2012.
- [5] Ii, S., Gong, X., Sugiyama, K., Wu, J., Huang, H. and Takagi, S., A full Eulerian fluid-membrane coupling method with a smoothed volume-of-fluid approach, *Comm. Comput. Phys.*, **12**, 544–576, 2012.
- [6] Ii, S., Sugiyama, K., Takagi, S. and Matsumoto, Y., A computational blood flow analysis in a capillary vessel including multiple red blood cells and platelets, *J. Biomech. Sci. Eng.*, **7**, 72–83, 2012.
- [7] Ohwada, T. and Asinari, P., Artificial compressibility method: asymptotic numerical method for incompressible Navier-Stokes equations, *J. Comput. Phys.*, **229**, 1698–1723, 2010.